Analysis of The Cross Section of Inkjet-Printed Conductive Tracks on PET Films

A method to analyze the nano- and microstructure of inkjet-printed conductive tracks on polymer film substrates based on SEM analysis of cross sections prepared by ultramicrotomy.

Martin Ungerer[1], Waldemar Spomer[1], Lisa Veith[3], Annika Fries[1], Christian Debatin[1], Irene Wacker[2], Rasmus Schröder[2,3], Ulrich Gengenbach[1]

[1] Institute for Applied Computer Science (IAI), Karlsruhe Institute of Technology (KIT), Eggenstein-Leopoldshafen, Germany

[2] Centre for Advanced Materials (CAM), University Heidelberg, Heidelberg, Germany

[3] CellNetworks, BioQuant, University Hospital Heidelberg, Heidelberg, Germany

e-mail: ungerer@kit.edu

***Abstract*—The development of internet of things devices, smart sensor systems or wearables necessitates new fabrication technologies. The challenge is to fulfil requirements such as flexibility, low-weight and low-cost. Inkjet printing of conductive microstructures on polymer films has become increasingly important for these applications in the last decade. This additive fabrication approach is potentially more ecofriendly than conventional processes but has still not reached wider implementation in industry. One of the potential reasons is the still insufficient reliability of printed components that must sustain electrical, thermal, mechanical and chemical stress. In order to optimize the fabrication process with regard to these requirements, the nano- and microstructure of printed patterns needs to be analyzed. In the present work, a method is outlined for the nano- and microstructure analysis of inkjet-printed conductive tracks on polymer substrates by means of scanning electron microscopy of cross sections prepared by ultramicrotomy.**

Keywords-Inkjet-printing; silver nanoparticle ink; polyethylene terephthalate; sintering; ultramicrotomy; imaging by scanning electron microscopy; cross section; microstructure; nanoparticle density.

I. INTRODUCTION

In the last decade, printing technologies have become more and more important in research and development for flexible electronics [1]. The objective is to replace conventional subtractive fabrication processes of printed circuit board (PCB) manufacturing by additive processes. Printing processes can be used to fabricate conductive structures, as well as more complex electronic components on flexible polymer films.

A. Advantages of printing technologies

Various printing technologies were transferred from the realm of graphic printing to electronics manufacturing in the last decade. As manufacturing processes can be divided into those, which are well suited for mass production and those that are more suited for single part or small series production, printing processes may be also classified with regard to process productivity. Conventional printing processes based on printing forms are well suited for large-scale production whereas non-impact principles are more suited to individual part up to small series manufacturing and research applications [2] [3].

Unlike the conventional fabrication of PCB's that needs some complex electroplating, lithography and etching steps, printing processes usually need one single additive fabrication step followed by an additional curing process in order to create conductive tracks on a substrate [4] [5]. Thus material usage is optimized and the toxic waste accumulated in subtractive processing is eliminated [6]. Printing allows faster, cleaner, cheaper and more environmentally friendly fabrication of PCB's than conventional processes [5]. Additionally, printing enables large area processing of flexible polymer substrates at low temperatures and ambient conditions [7].

The implementation of printing processes for a desired electronic function in microstructure resolution demands prudent selection of the three main process components - ink, substrate and printing system. These components have to be precisely tuned to get optimum conditions for realizing features with high reproducibility [2].

B. Conductive ink

A fundamental element in printed electronics are conductive tracks [4]. They have to provide high conductivities in order to minimize the power loss. Regarding this requirement, currently two main ink types are available. One type are metal organic decomposition (MOD) inks, with oxidized metal ions as main component [8]. The most prevalent type are nanoparticle inks, where the particles are dispersed in solvents and stabilized by an organic capping agent against agglomeration [9].

Due to their high conductivity, silver-based inks are most widely used in this context [6]. For printed silver nanoparticle tracks a conductivity of about 10 % of bulk silver is acceptable for many applications [10].

The nanoparticle size severely influences the curing process. The smaller the particles, the lower the melting point compared to the bulk material [11] [12].

 ISBN: 978-1-61208-538-8

C. Substrate

For printed flexible electronic applications with optical functions, often low cost polyethylene terephthalate (PET) substrates are used which have a glass-transition temperature (T_g) of 78 °C and a melting point of 255 °C [13] [14]. Commercially available PET films, e.g., Melinex® ST from DuPont Teijin Films are often used in printed electronic applications. Such PET substrates are thermoplastic semi-crystalline polymer films whose maximum working temperature for printing and sintering processes (T_{max}) from about 150 °C is largely independent of their T_g due to a heat-stabilization [13] [14] [15]. Semi-crystalline polymer films have better resistances against solvents than amorphous polymers [15].

D. Inkjet-printing

Drop-on-demand (DoD) piezo inkjet printing is the most common non-impact printing principle in the field of printed electronics [7]. It allows direct, mask-less and vectorial printing of layouts on flexible polymer films [2]. The layouts are created by computer-aided design (CAD). With regard to printability, ink property parameters such as viscosity, surface energy, density, particle size and particle stability are of crucial importance [4] [5]. For example, a particle size of less than 100 nm is recommended in order to prevent print head nozzle clogging [16].

Compared to conventional electronics fabrication processes, inkjet-printed structures often suffer from non-uniformity, low line edge quality and non-reproducible morphology [17] [18]. In order to obtain an optimum line quality, the important parameters that need to be controlled are the distance between two adjacent droplets (d_d), the frequency of droplet generation (f_d), the droplet velocity (v_d), the substrate temperature (T_s) and substrate surface properties [19] [20].

E. Curing

After the printing process, the resulting structures must be cured in order to get the desired electrical conductivity [10]. First, the ink solvent has to be evaporated; then, the organic stabilizing shell has to be removed. During the sintering, a percolation-based network of conductive paths is established due to sporadic agglomeration of particles [10]. At higher temperatures, sintering necks improve the conductivity, the coalescence of the particles leads to a higher metal density of the printed feature [21]. High conductivities have been achieved by means of an oven sintering regime with 30 minutes or more at temperatures above 250 °C [1].

Despite the lower melting point of nanoparticles compared to the bulk material, a sintering regime required for such an enhanced conductivity is not compatible with many of the preferably used low-cost polymer substrates, e.g., PET [22].

Therefore, low temperature sintering methods are taken into consideration that allow either sintering at room temperature (commonly known as chemical sintering) or selective sintering where only the printed structure that needs to be cured is heated while the substrate stays at moderate temperatures [1].

Chemical sintering comprises, among other methods, sintering triggered by additives in the ink or in the substrate [23].

Selective sintering methods are photonic flash sintering, laser sintering, plasma sintering, microwave sintering and electrical current sintering [1] [10].

F. Properties of printed structures

In view of the manifold applications of printed structures, such as conductors, passive components, etc., not only their electrical characteristics must be considered, but also their mechanical and chemical properties. Printed conductive tracks have to withstand mechanical, chemical und thermal stresses that can influence their inherent porous nanostructure and thereby impair the reliability. Particularly, adhesion strength to the substrate, bendability and fatigue resistance are important properties of printed structures for applications on flexible polymer substrates. Sintering conditions substantially influence mechanical properties, such as fatigue resistance [24].

G. Hybrid electronics

To date, many electronic functional elements besides conductive tracks such as resistors, capacitors, transistors, organic light emitting diodes (OLED), organic photovoltaics (OPV) and sensors have been realized by printing technologies. However, it is currently not possible to achieve the performance of conventionally fabricated devices. Moreover, highly integrated circuits such as microcontrollers cannot yet be realized by printing. Therefore, a hybrid approach for the fabrication of more complex electronic systems on flexible polymer substrates seems to be an interesting solution in the medium term to overcome the still low performance of printed complex elements [25] [26]. Marjanović et al. define hybrid electronic integration as the combination of printed components and surface-mount technology (SMT) devices on foils [25].

For demonstration of a hybrid intralayer-integration approach, the conductive track structure of a flip-flop circuit shown in [26] was first printed via silver nanoparticle ink on a PET film. Then SMT components were mounted with conductive adhesive. Figure 1 shows the realized flip-flop

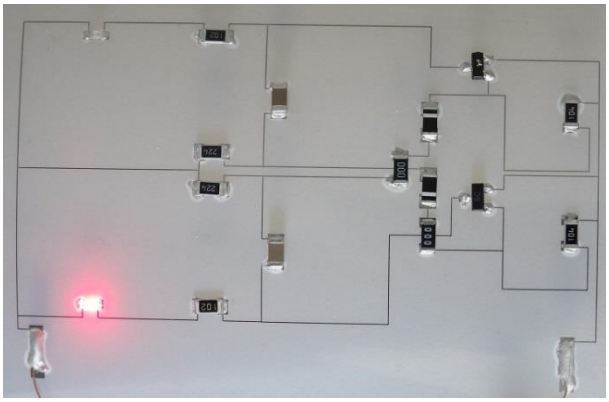

Figure 1. Flip-flop circuit with printed conductive tracks and mounted SMT-components

circuit. Tests with such circuits indicated that the system is sensitive to mechanical stress such as bending. Either the conductive adhesive that connects the SMT components fails or the conductive tracks crack or delaminate from the substrate. In order to improve the structure's resistance to mechanical stress, the microstructure of the printed tracks has to be investigated, as it directly affects the mechanical properties of the printed feature and is of high importance for reliable circuits [27].

After this introduction to hybrid electronics using additive manufacturing processes, in section II the materials and methods are described that were used for realizing test structures. In section II A., the test structure is described, in II B., the applied inkjet printer, the silver ink and the PET substrate are presented. The Section II C. illustrates the printing process and II D. the sample preparation that is needed for the analysis of the cross sections. In section III, the results of the printing process (III A.), the sample preparation (III B.) and the SEM analysis of the fabricated cross sections (III C.) are outlined. Finally, section IV gives a conclusion and an outlook.

II. MATERIALS AND METHODS

A. Test structure

A test structure was defined for the electrical and mechanical evaluation of the properties of different ink-substrate-printer-combinations and different processing parameters. The test structure conceived for electrical and mechanical characterization consists of a 45 mm long conductive track (L) that connects two contact pads each having a length (B) of 7 mm and a width (T) of 2 mm. Figure 2 shows the geometry of the test structure (top) and some inkjet-printed samples (bottom).

B. Material (printer, ink and substrate)

The printer used for printing the test structures is based on our custom-built piezo-driven four-axis positioning system NAMOSE. It has a working space of 400 mm x 150 mm x 40 mm, a repeatability of less than 1 µm and a maximum speed of 200 mm/s [2]. NAMOSE is controlled by a Beckhoff-CX2040 with TwinCAT, programmable logic controller (PLC) and numerical control (NC) axis controlling. For inkjet-printing, the positioning system is equipped with a piezo-electrically driven single nozzle Microfab print head (MJ-AL-01-50-8MX) with an orifice diameter of 50 µm [2]. A NC-task synchronizes the droplet frequency (f_d) with the axis velocity (v), while the droplet distance (d_d) is maintained at its set point. Furthermore, the NAMOSE is equipped with a heated vacuum chuck and an optical observation system for controlling and adjusting droplet formation.

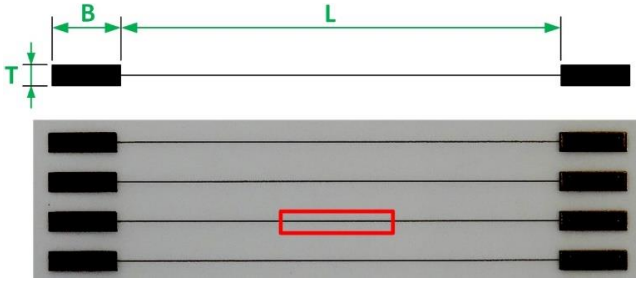

Figure 2. Inkjet test structure. Geometry (top), image of printed test structures (bottom), specimen geometry for ultramicrotomy (red box)

The silver-nanoparticle ink DGP 40LT-15C (Advanced Nano Products (ANP)) was purchased from Sigma Aldrich (736465 ALDRICH). The ink has a solid content of 30 - 35 wt %, a surface tension of 35 - 38 mN/m, a viscosity of about 10 - 17 mPa·s and is designed for application on polymer films. The manufacturer recommends a curing regime with 30 - 60 minutes at 120 - 150 °C. The main solvent of the ink is triethylene glycol monoethyl ether (TGME) [28]. The ink contains polyvinylpyrrolidone (PVP) as capping agent that leads to an electrostatic stabilization of the nanoparticles [9].

In the present work, two different PET-films were used as substrates. The 125 µm thick Melinex® ST506™ from DuPont Teijin Films is optimized for printed electronics. Both sides of this film are pre-treated for improved adhesion of inks [14]. The NB-TP-3GU100 from Mitsubishi Paper Mills is a 135 µm thick PET-film that is optimized for inkjet-printing of conductive structures based on silver nanoparticle dispersions. Due to its optimized nanoporous single side coating, it provides fast drying of water-based inks [29]. The thickness, morphology and the surface chemistry of this coating are not further specified by the supplier.

C. Printing samples

Test structures were printed on both substrates using the ink DGP 40LT-15C. Table I shows the printing parameters for four different samples. After printing, the samples were cured in a convection oven (Memmert UP 500) for about 60 min. at 120 °C.

After curing, the width of the central part of the test structure (see the red box in Figure 2) was measured by optical microscopy and image processing with the DIPLOM software that was developed at the KIT Institute for Applied Computer Science (IAI). The image processing yields the standard deviation of the line widths, which can be used as indicator of the line edge quality.

D. Sample preparation for SEM-analysis

For analyzing the cross section of central printed tracks, about 10 mm long and 1.5 mm wide rectangular specimen were cut from the printed test structures (see the red box in Figure 2).

As it is not possible at ambient conditions, to directly cut the flexible polymer with an ultramicrotome without

TABLE I. PRINTING PARAMETERS

sample	substrate	d_d [µm]	T_S [°C]	v [mm/s]
A	Melinex® ST506™	147	80	50
B	Melinex® ST506™	13	80	50
C	NB-TP-3GU100	31	RT	10
D	NB-TP-3GU100	1	RT	10

 ISBN: 978-1-61208-538-8

delamination of the ink, the printed samples need to be embedded into polymer blocks in order to get appropriate sections. Two different specimens were embedded parallel to each other into one embedding mould.

As embedding resin, the Embed 812 Kit from Electron Microscopy Sciences was used. The filled embedding moulds were cured over night at 60 °C in a convection oven.

After polymerization, the blocks with the embedded samples were removed from the moulds and then prepared for ultramicrotomy. For this purpose, the blocks were trimmed in a Leica Ultracut 7 ultramicrotome using a standard glass trimming knife. Then, sections of 100 nm and 200 nm thickness were cut with the same instrument but with a Diatome Ultra 35° knife at ambient conditions. The knife boat was filled with double-distilled water during the cutting process. To avoid electrostatic charging of the sample, a Diatome static line 2 ionizer was used. The cut sections are floating on the water surface of the knife boat, where they can be subsequently picked up and placed on a silicon wafer for imaging in the scanning electron microscope (SEM).

For SEM imaging, an Ultra 55 (Carl Zeiss Microscopy, Oberkochen, Germany) was used.

Particle density in the SEM images of the cross sections was measured with the software package Fiji [30]. Figure 3 illustrates the approach to determine the particle density by image segmentation. The threshold for the segmentation was manually selected for different details of a SEM-image of a cross section. The density of the particles in the sectional plane was calculated for each detail.

III. Results and Discussion

A. Printing

In a preliminary test, it was found that the behavior of the ink after deposition at room temperature is completely different on the two different substrates. Although the initial wetting seems to be good, printing on the Melinex® ST506™ substrate is followed by a continuous parasitic spreading combined with a resulting shape similar to a coffee-ring effect. This results in very flat, broad and fringed tracks, with poor edge qualities. The nanoporous coating of the PET-film from Mitsubishi Paper Mills avoids this ink spreading over a broad range of droplet-distances d_d. A considerable track

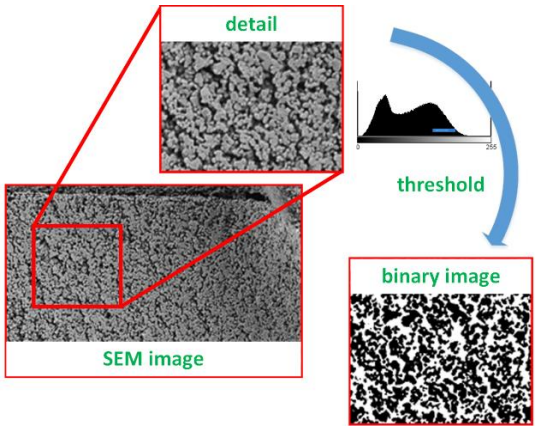

Figure 3. Determination scheme of the nanoparticle density

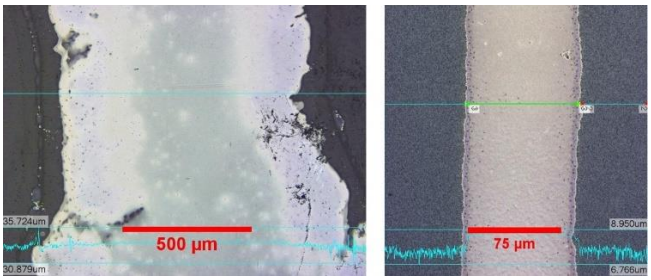

Figure 4. Microscope images of printed silver ink tracks at room temperature on Melinex® ST506™ (left) and on NB-TP-3GU100 (right)

height can be achieved, even for narrow tracks. Optimizing the droplet-distance (d_d), it is even possible to print continuous tracks with a width of less than the diameter of a single droplet. Figure 4 shows microscope images of this preliminary test. The printing parameters were the same for both substrates: the jetting frequency (f_d) was 2000 Hz, the axis speed (v) was 100 mm/s and the droplet-distance (d_d) results in 50 µm. The silver track on Melinex® ST506™ (see Figure 4 left) shows a poor edge quality, a width of about 1180 µm and a height in the range of about 100 nm, whereas the line printed on NB-TP-3GU100 (see Figure 4 right) has a good edge quality at a width of about 88 µm and a height of about 1140 nm.

In further tests, it was found that printing on Melinex® ST506™, with 80 °C substrate temperature results in much better track quality. This parameter was maintained for all subsequent tests with this substrate.

Concerning the sintering in a convection oven, an irreversible bulging of the NB-TP-3GU100 can be observed when heating above T_g of PET. A possible explanation for this effect could be different thermal expansion coefficients of the single-side nanoporous coating and the PET bulk material. The Melinex® ST506™ foil does not show such an effect.

B. Sample preparation via ultramicrotomy

Figure 5 shows the block with the embedded specimens (left, a and b), the top of the block during trimming with the glass knife (center, c) and a section directly after cutting (right).

200 nm sections can be cut reproducibly but with a significant wrinkling of the embedded specimens in the sections (see Figure 5 right, d and e). Lower section

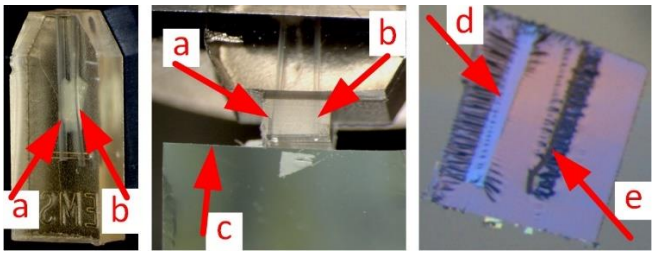

Figure 5. Sample preparation via ultramicrotomy. Embedded specimens (a and b), trimming (center) with a glass knife (c) and 200 nm thin section floating on the water in the knife boat (right); Wrinkling at the embedded specimen (d and e)

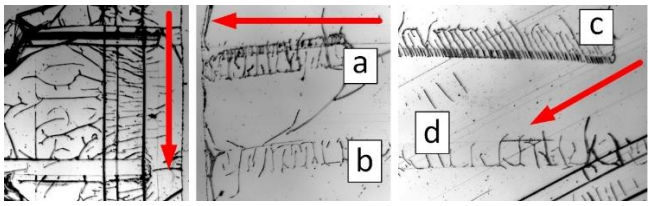

Figure 6. Influence of the cutting direction on the section morphology and the specimens (a and c: NB-TP-3GU100; b and d: Melinex® ST506™). Perpendicular (left), parallel (center) and 26° (right) to substrate plane (arrows indicate cutting direction)

thicknesses led to delamination between specimen and embedding resin.

An initial observation of the cross sections concerned the nanoporous coating of the Mitsubishi substrate: We found a 35 µm thick layer. The high thickness of this layer supports the hypothesis stated above that this might be the main reason for the warping of the substrate after thermal sintering.

Different cutting directions were tested with respect to the sample orientation in the block: perpendicular, parallel and at an angle to the embedded substrate plane. Figure 6 shows typical results indicating the effect of the cutting direction (red arrows).

When cutting is performed perpendicular to the substrate plane, the interface between the ink and the substrate is compressed and can therefore not be used for further investigation of the interface. Additionally, this section shows many wrinkles and dominant knife marks (see Figure 6 left). In contrast, sections obtained when cutting parallel to the substrate plane, show less wrinkles and knife marks (see Figure 6 center). It is assumed that this cutting direction introduces fewer mechanical stresses to the interface between ink and substrate. The sections obtained, when cutting at an angle of about 26° to the substrate plane, were also acceptable (see Figure 6 right). The embedded NB-TP-3GU100 substrate (see Figure 6 a and c) produces much more wrinkles than the Melinex® ST506™ (see Figure 6 b and d). We suppose that Melinex® film is harder than the Mitsubishi film due to its heat and surface treatment. This can

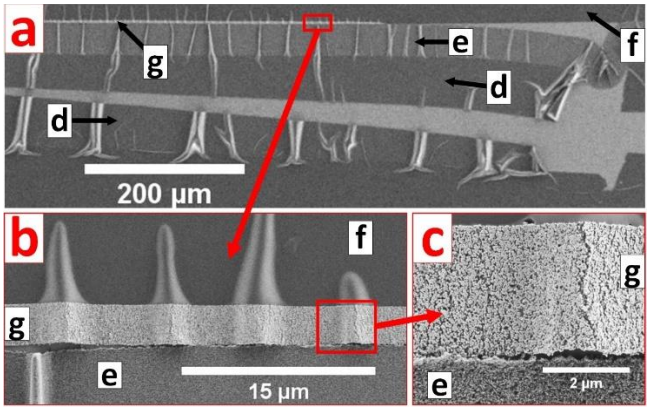

Figure 7. SEM images of a section containing a silver track (g) printed on NB-TP-3GU100 substrate (d: bulk, e: nanoporous coating, f: embedding resin); low magnification (a), high magnification (b, c); bulk substrate delamination (a); cracks and delamination of conductive cracks (b, c)

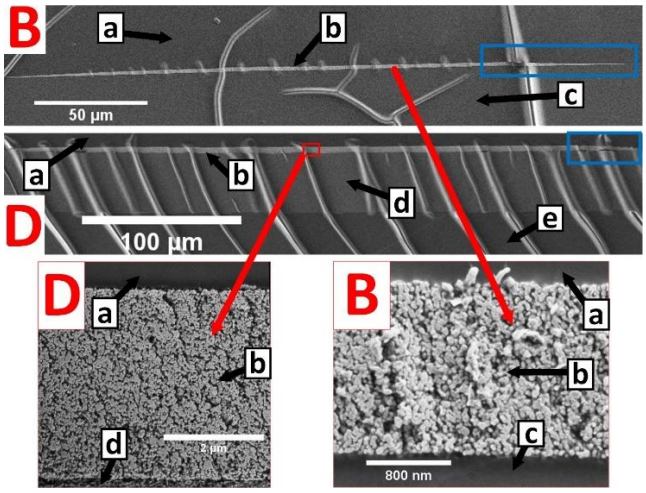

Figure 8. SEM images of sections containing the samples B (a: embedding resin, b: silver ink, c: substrate) and D (a: resin, b: silver ink, d: nanoporous coating, e: bulk substrate); low magnification (top) and high magnification images (bottom)

explain why the sections of NB-TP-3GU100 specimen show a stronger wrinkling than the Melinex® substrate.

C. SEM analysis and image segmentation

Despite varying the cutting direction, a certain degree of section wrinkling was unavoidable. This led to a degradation of the sections in terms of cracks. Sometimes delamination occurred in the section while cutting. Figure 7 shows a section from a NB-TP-3GU100 substrate cut parallel to the substrate plane (a). It can be seen that the substrate was torn during the cutting process (see Figure 7 a) and the printed ink delaminates from the coated substrate at the locations of the wrinkles (b and c).

Nevertheless, there are enough regions suitable for further analysis (compare Figure 7 b and c), since the cutting preserved the nanostructure of the cross section.

Figure 8 shows the cross section of the samples B and D. The full low magnification cross section for each sample can be seen on the top, a detail image can be found on the bottom for each sample. Using such high magnification images from SEM we determined the particle density of each sample according to the procedure described above. The particle density of the conductive tracks calculated for all four samples was between 58 % and 65 %.

Additionally, we found that the cross section of the tracks printed on Melinex® ST506™ levels off continuously in the direction of the edges (see the blue box in Figure 8 B). In contrast, the height of the silver track on NB-TP-3GU100 only decreases close to the edges (see the blue box in Figure 8 D).

IV. Conclusion and Outlook

A method was outlined for analyzing the nano- and microstructure of inkjet printed conductive tracks on different polymer substrates using ultramicrotomy. The sections produced showed wrinkling along the substrate plane partially leading to delamination. This may result from stiffness differences between the substrate material and the

embedding resin, a parameter to be optimized in further investigations. Despite these delaminations, there were sufficient regions that could be used for investigation of the nanoparticle network of the printed conductive tracks. This indicates that with properly optimized embedding and cutting parameters, the described scheme is a promising method for analyzing thermal, mechanical and chemical influences on the nanostructure of printed metal nanoparticle inks and on the interface between substrate and ink.

ACKNOLEDGMENTS

The authors thank Dr. Tim Scharnweber from the KIT Institute for Biological Interfaces (IBG1) for enabling the measurements with the laser-scanning microscope.

REFERENCES

[1] J. Perelaer, and U. S. Schubert. "Novel approaches for low temperature sintering of inkjet-printed inorganic nanoparticles for roll-to-roll (R2R) applications," Journal of Materials Research, vol. 28, pp. 564–573, 2013, doi: 10.1557/jmr.2012.419.

[2] M. Ungerer, U. Gengenbach, A. Hofmann, and G. Bretthauer. "Comparative and systemic analysis of digital single nozzle printing processes for the manufacturing of functional microstructures," Proc. MikroSystemTechnik Kongress (MST 2015): MEMS, Mikroelektronik, Systeme, Oct. 2015, ISBN: 978-3-8007-4100-7.

[3] J. Lessing et al. "Inkjet Printing of Conductive Inks with High Lateral Resolution on Omniphobic “RF Paper” for Paper-Based Electronics and MEMS," Advanced Materials, vol. 26, pp. 4677–4682, 2014, doi: 10.1002/adma.201401053.

[4] H.-H. Lee, K.-S. Chou, and K.-C. Huang. "Inkjet printing of nanosized silver colloids," Nanotechnology, vol. 16, p. 2436, 2005, doi: 10.1088/0957-4484/16/10/074.

[5] Y. Kawahara, S. Hodges, N.-W. Gong, S. Olberding, and J. Steimle. "Building Functional Prototypes Using Conductive Inkjet Printing," IEEE Pervasive Comput., vol. 13, pp. 30–38, 2014, doi: 10.1109/MPRV.2014.41.

[6] T. Öhlund et al. "Assisted sintering of silver nanoparticle inkjet ink on paper with active coatings," RSC Advances, vol. 5, pp. 64841–64849, 2015, doi: 10.1039/C5RA06626C.

[7] S. H. Ko et al. "All-inkjet-printed flexible electronics fabrication on a polymer substrate by low-temperature high-resolution selective laser sintering of metal nanoparticles," Nanotechnology, vol. 18, p. 345202, 2007, doi: 10.1088/0957-4484/18/34/345202.

[8] J. Perelaer et al. "Plasma and Microwave Flash Sintering of a Tailored Silver Nanoparticle Ink, Yielding 60% Bulk Conductivity on Cost-Effective Polymer Foils," Advanced Materials, vol. 24, pp. 3993–3998, 2012, doi: 10.1002/adma.201200899.

[9] H. Andersson et al. "Inkjet Printed Silver Nanoparticle Humidity Sensor With Memory Effect on Paper," IEEE Sensors J., vol. 12, pp. 1901–1905, 2012, doi: 10.1109/JSEN.2011.2182044.

[10] J. Niittynen et al. "Alternative sintering methods compared to conventional thermal sintering for inkjet printed silver nanoparticle ink," Thin Solid Films, vol. 556, pp. 452–459, 2014, doi: 10.1016/j.tsf.2014.02.001.

[11] G. L. Allen, R. A. Bayles, W. W. Gile, and W. A. Jesser. "Small particle melting of pure metals," Thin Solid Films, vol. 144, pp. 297–308, 1986, doi: 10.1016/0040-6090(86)90422-0.

[12] P. Buffat, and J.-P. Borel. "Size effect on the melting temperature of gold particles," Phys. Rev. A, vol. 13, p. 2287, 1976, doi: 10.1103/PhysRevA.13.2287.

[13] W. A. MacDonald. "Engineered films for display technologies," J. Mater. Chem., vol. 14, p. 4, 2004, doi: 10.1039/b310846p.

[14] DuPont Teijin Films. "Product Information Melinex® ST506™," [Online]. Available from: http://www.koenig-kunststoffe.de/produkte/melinex/melinex-r-st506.pdf, [retrieved: Feb, 2017].

[15] W. A. MacDonald et al. "Latest advances in substrates for flexible electronics," Journal of the Society for Information Display, vol. 15, pp. 1075–1083, 2007, doi: 10.1889/1.2825093.

[16] U. Caglar, K. Kaija, and P. Mansikkamaki. "Analysis of mechanical performance of silver inkjet-printed structures," Proc. IEEE 2nd International Nanoelectronics Conference (INEC 2008), Mar. 2008, pp. 851–856, ISBN: 978-1-4244-1572-4, doi: 10.1109/INEC.2008.4585617.

[17] D.-H. Lee, K.-T. Lim, E.-K. Park, J.-M. Kim, and Y.-S. Kim. "Optimized ink-jet printing condition for stable and reproducible performance of organic thin film transistor," Microelectronic Engineering, vol. 111, pp. 242–246, 2013, doi: 10.1016/j.mee.2013.03.177.

[18] G. Li, R. C. Roberts, and N. C. Tien. "Interlacing method for micro-patterning silver via inkjet printing," Proc. IEEE 13th Sensors Conference, Nov. 2014, pp. 1687–1690, ISBN: 978-1-4799-0162-3, doi: 10.1109/ICSENS.2014.6985346.

[19] F. Molina-Lopez, D. Briand, and N. F. de Rooij. "All additive inkjet printed humidity sensors on plastic substrate," Sensors and Actuators B: Chemical, 166–167, pp. 212–222, 2012, doi: 10.1016/j.snb.2012.02.042.

[20] D. Soltman, and V. Subramanian. "Inkjet-printed line morphologies and temperature control of the coffee ring effect," Langmuir the ACS journal of surfaces and colloids, vol. 24, pp. 2224–2231, 2008, doi: 10.1021/la7026847.

[21] I. Reinhold et al. "Argon plasma sintering of inkjet printed silver tracks on polymer substrates," Journal of Materials Chemistry, vol. 19, pp. 3384–3388, 2009, doi: 10.1039/B823329B.

[22] J. Perelaer, M. Klokkenburg, C. E. Hendriks, and U. S. Schubert. "Microwave Flash Sintering of Inkjet-Printed Silver Tracks on Polymer Substrates," Advanced Materials, vol. 21, pp. 4830–4834, 2009, doi: 10.1002/adma.200901081.

[23] S. Magdassi, M. Grouchko, O. Berezin, and A. Kamyshny. "Triggering the sintering of silver nanoparticles at room temperature," ACS nano, vol. 4, pp. 1943–1948, 2010, doi: 10.1021/nn901868t.

[24] B.-J. Kim et al. "Improving mechanical fatigue resistance by optimizing the nanoporous structure of inkjet-printed Ag electrodes for flexible devices," Nanotechnology, vol. 25, p. 125706, 2014, doi: 10.1088/0957-4484/25/12/125706.

[25] N. Marjanović. "Hybrid electronics systems by CSEM," Proc. 8th International Exhibition and Conference for the Printed Electronics Industry (LOPEC 2016): Technical Conference, München, Apr. 2016.

[26] U. Gengenbach et al. "A toolbox for multifunctional multilayer printed systems," Proc. MikroSystemTechnik Kongress (MST 2015): MEMS, Mikroelektronik, Systeme, Oct. 2015, ISBN: 978-3-8007-4100-7.

[27] S. Merilampi, T. Laine-Ma, and P. Ruuskanen. "The characterization of electrically conductive silver ink patterns on flexible substrates," Microelectronics Reliability, vol. 49, pp. 782–790, 2009, doi: 10.1016/j.microrel.2009.04.004.

[28] Advanced Nano Products (ANP). "Nano-Silver Ink for Inkjet Printing," [Online]. Available from: http://anapro.com/eng/product/silver_inkjet_ink.html, [retrieved: Feb, 2017].

[29] Mitsubishi Paper Mills. "Technical Data Sheet: Mitsubishi Nano Benefit Series NB-TP-3GU100," [Online]. Available from: https://www.mitsubishi-paper.com/fileadmin/user_upload/PrePress/downloads/silver_nano/PET_Film_NB-TP-3GU100.pdf, [retrieved: Feb, 2017].

[30] J. Schindelin et al. "Fiji: an open-source platform for biological-image analysis," Nature Methods, vol. 9, pp. 676–682, 2012, doi: 10.1038/nmeth.2019.

 ISBN: 978-1-61208-538-8